

AUTHOR QUERIES

AUTHOR PLEASE ANSWER ALL QUERIES

PLEASE NOTE: We cannot accept new source files as corrections for your article. If possible, please annotate the PDF proof we have sent you with your corrections and upload it via the Author Gateway. Alternatively, you may send us your corrections in list format. You may also upload revised graphics via the Author Gateway.

Carefully check the page proofs (and coordinate with all authors); additional changes or updates WILL NOT be accepted after the article is published online/print in its final form. Please check author names and affiliations, funding, as well as the overall article for any errors prior to sending in your author proof corrections.

- 1) Please be aware that authors are required to pay overlength page charges (\$230 per page) if the article is longer than 3 pages. If you cannot pay any or all of these charges please let us know. GRS Society members receive a discounted rate of \$200 per page.
- 2) This pdf contains 2 proofs. The first half is the version that will appear on Xplore. The second half is the version that will appear in print. If you have any figures to print in color, they will be in color in both proofs.
- 3) The “Open Access” option for your article expires when the article is published on Xplore in an issue with page numbers. Articles in “Early Access” may be changed to Open Access. If you have not completed your electronic copyright form (ECF) and payment option please return to Scholar One “Transfer Center.” In the Transfer Center you will click on “Manuscripts with Decisions” link. You will see your article details and under the “Actions” column click “Transfer Copyright.” From the ECF it will direct you to the payment portal to select your payment options and then return to ECF for copyright submission.

AQ:1 = Please confirm or add details for any funding or financial support for the research of this article.

AQ:2 = Please confirm the location and postal codes for Federal University of São Carlos and John Deere.

AQ:3 = Please provide the publisher name and publisher location for Ref. [1].

Productive Crop Field Detection: A New Dataset and Deep-Learning Benchmark Results

Eduardo Nascimento[✉], John Just, Jurandy Almeida[✉], and Tiago Almeida[✉]

Abstract—In precision agriculture, detecting productive crop fields is an essential practice that allows the farmer to evaluate operating performance separately and compare different seed varieties, pesticides, and fertilizers. However, manually identifying productive fields is often time-consuming, costly, and subjective. Previous studies explore different methods to detect crop fields using advanced machine-learning (ML) algorithms to support the specialists' decisions, but they often lack good quality labeled data. In this context, we propose a high-quality dataset generated by machine operation combined with Sentinel-2 images tracked over time. As far as we know, it is the first one to overcome the lack of labeled samples by using this technique. In sequence, we apply a semisupervised classification of unlabeled data and state-of-the-art supervised and self-supervised deep-learning (DL) methods to detect productive crop fields automatically. Finally, the results demonstrate high accuracy in positive unlabeled (PU) learning, which perfectly fits the problem where we have high confidence in the positive samples. Best performances have been found in Triplet Loss Siamese given the existence of an accurate dataset and contrastive learning considering situations where we do not have a comprehensive labeled dataset available.

Index Terms—Crop field detection, machine learning (ML), precision agriculture.

I. INTRODUCTION

FOOD production needs to grow by 70% to meet the demands of the expected world population by 2050 [1]. Motivated by this challenge, agriculture has adopted technologies to improve and optimize input returns while preserving natural resources. Integrating these technologies promotes a farming management concept known as *precision agriculture* [2]. The main goal of precision agriculture is to provide tools for allowing the farmer to observe, measure, and respond to field variability in crops facilitating faster and better decisions. In addition, these techniques are generic enough to be applied to various crops, including but not limited to corn, soy, coffee, sugarcane, beans, and even pastures [3], [4].

To efficiently organize and manage large crops, farmers leverage remote sensing to divide their land into smaller observation units that this work will refer to as *agricultural* or

Manuscript received 18 May 2023; revised 6 July 2023; accepted 11 July 2023. (*Corresponding author: Eduardo Nascimento*.)

Eduardo Nascimento, Jurandy Almeida, and Tiago Almeida are with the Department of Computer Science, Federal University of São Carlos, São Paulo 13565-905, Brazil (e-mail: egnascimento@gmail.com; jurandy.almeida@ufscar.br; talmeida@ufscar.br).

John Just is with the Department of Data Science and Analytics, John Deere, Ames, IA 50011 USA (e-mail: johnpjst@gmail.com).

Digital Object Identifier 10.1109/LGRS.2023.3296064

crop fields. A field shape is designed based on topography and mechanization planning. For example, fields are built around contour farming and the ideal length to fill the wagon capacity in a sugarcane crop. The same logic is followed for grains in the Brazilian South and Southeast. Nonetheless, the most important variable is the harvester capacity in the Midwest, where the topography is often plain [5], [6], [7]. A *productive crop field* is an area consistently used for the cycle of growth and harvest of a crop, typically yearly but more often in some regions with favorable soil and weather.

Thanks to the availability of a massive amount of labeled data, the development of artificial intelligence (AI), particularly machine learning (ML) and deep learning (DL), has allowed for acceleration and improvement in many areas of agriculture [8], [9], [10], [11], [12]. Despite all the advances, having an adequate amount of labeled data to train such methods can be costly and not always affordable for precision farming.

Usually, farmers rely on experts to build the field boundaries in dedicated geographic information system (GIS) software. Despite the expert's ability and knowledge, finding crop fields and drawing their boundaries has been a major, expensive, and time-consuming challenge [13]. The larger the customer's land is, the more significant the number of fields to be created. For instance, there are farms in Brazil with more than 18 000 fields that require regular updates to reflect their accurate states. Finding productive fields is even more challenging because it requires previous knowledge of these areas or the analysis of satellite images over time.

Aiming to facilitate access to data ready to support ML and DL models for productive crop field detection, we introduce a new dataset of productive fields based on the agriculture machine's operation combined with Sentinel-2 images collected over a period of time. First, this information is aggregated in geospatial L12 hexagons, establishing a common ground for employing different satellite sources with different resolutions. Second, typical farmers are usually interested in monitoring productive areas rather than all possible fields since many are not fertile or suitable for any crop. For this purpose, the proposed dataset contains highly accurate positive samples (i.e., productive crop fields) and inferred negative ones, making it well-suited for positive and unlabeled learning [14]. Moreover, recent advances suggest that self-supervised methods (e.g., contrastive learning) may also provide a promising alternative even for cases where labeled samples are scarce [15]. Finally, we offer state-of-the-art ML

and DL benchmark results for further comparison, including classification methods with different training strategies (i.e., supervised learning, self-supervised learning, and semisupervised classification of unlabeled data).

II. RELATED WORK

Automatically detecting productive crop fields is a challenge that intersects multiple areas, and its solution could fill important gaps in agriculture management and environment control [7]. In this context, Crommelinck et al. [16] have worked on boundary detection of agricultural fields to provide automated recording of land rights, a slightly different purpose despite sharing common problems. However, despite the proven benefits of fully automated boundary detection and the research already accomplished, it is still considered an open problem with significant innovation opportunities, especially when sufficient training data is unavailable [12], [17].

North et al. [18] used classical computer vision techniques to detect the boundaries of farm fields in New Zealand. However, their technique resulted in only 59% accuracy, which is insufficient for most applications. Moreover, their strategy is highly impacted by variations caused by the season in the images extracted. Still based on classic computer vision, Evans et al. [19] used a region-based technique called canonically guided region growing to segment multispectral images and, despite being more accurate than previous work, it was applied to a very small and manually annotated set of images requiring further investigation in a more broad collection of samples.

Since classical computer vision techniques alone are often insufficient to achieve good results, further research evaluated ML models to detect crop boundaries. For instance, García-Pedrero et al. [20] achieved an accuracy of 92% using an ensemble algorithm called RUSBoost [21] to merge superpixels and group blocks of the image, which were part of the same field. This study demonstrated how ML is a promising alternative and a precursor to further development using DL [20]. In the same year, Kussul et al. [22] applied DL to segment and classify crop types. They demonstrated the advantages of deeper networks by comparing a multilayer perceptron (MLP) with a convolutional neural network (CNN), where the latter achieved higher accuracies. Later, García-Pedrero et al. [8] applied the U-Net, a CNN for semantic image segmentation, to perform the same task with improved performance [8], [20], [23].

Concurrently, Persello et al. [9] designed a DL approach using SegNet, a CNN commonly used for semantic segmentation in very high-resolution (VHR) images. In this work, some significant mistakes were generally associated with poor-quality training data [9]. The authors extend their work to medium-resolution images from Sentinel-2; however, they observed a severe limitation during training since the employed methods comprised many convolutional layers resulting in a time-consuming task [9], [10].

Wagner and Oppelt [13] designed a modified version of the growing snakes active contour model based on graph theory concepts [13]. In sequence, Wagner and Oppelt [24] integrated

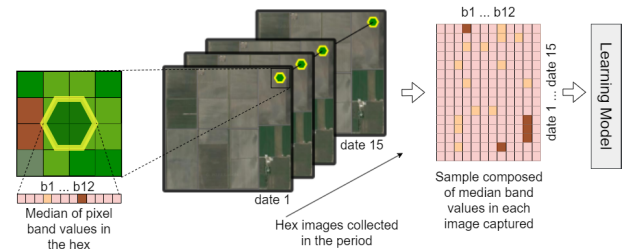


Fig. 1. Sequence to build a sample based on the hexagon time series.

a DL approach into their already proven graph-based model. The method achieved high results in rural areas but required further investigation of the missed boundaries, especially in areas closer to the cities [13], [24].

Waldner and Diakogiannis [11] compared DL methods, starting with ResUNet-a and followed by an improvement named Fractal-ResUNet, a network designed for semantic segmentation of agricultural images. The best accuracies were achieved with Sentinel-2 images, and it is considered state-of-the-art in boundary detection of agricultural fields. However, it depends on a large amount of training data with high-quality labeling to achieve consistent results [11], [12].

Most aforementioned studies were devised for detecting or segmenting all possible fields, regardless of whether they are productive. Only a few consider productive fields, but even these disregard their eventual changes over time.

III. PRODUCTIVE FIELDS DATASET

The dataset is stored in a tabular format, where each row corresponds to a hexagon, along with a timestamp and satellite band values. The hexagon format was used for geoanalysis since it facilitates storing and modeling spatiotemporal data from multiple disparate sources while avoiding using rasters. We used the H3 Python library¹ to create such hexagons with a level of L12. At this level, each hexagon has edges of approximately 10 m, resulting in a hexagonal area that covers 307 m², slightly bigger than three Sentinel-2 pixels. This resolution offers a balanced tradeoff between granularity and computational efficiency while training the models. Moreover, hexagons of this size can capture fine-grained variations in satellite data within a manageable dataset size, enabling efficient processing and analysis.

The timestamps are associated with the date and time the Sentinel-2 images were captured, providing temporal information. There are images from 2018-10-29 17:04:21 to 2019-08-15 16:59:01. Finally, the 12 band values correspond to the pixel median values in the area covered by that particular H3 hexagon. With this, we can summarize the satellite data for each hexagon in a compact and interpretable format, facilitating downstream ML analyses. Fig. 1 illustrates how we create the samples used as the input for the learning models.

Table I summarizes the dataset and its fields. The dataset includes 17 productive corn crop fields in the US within the same geographical area. It has 106 735 rows, each representing a hexagon captured on a specific date and time, followed by

¹The H3 Python library is available at <https://pypi.org/project/h3/>. Access on May 4, 2023.

TABLE I
PRODUCTIVE FIELDS DATASET DESCRIPTION

Fields: 17					
	Hexes (samples)		Hex images collected in the period		
Field	positive	negative	positive	negative	average
F01	558	210	9,860	3,539	17.67 ± 0.48
F02	734	151	14,242	2,863	19.40 ± 0.74
F03	59	85	1,075	1,528	18.22 ± 0.65
F04	350	150	8,326	3,518	23.79 ± 0.48
F05	75	134	1,815	3,001	24.20 ± 0.90
F06	288	60	4,999	1,044	17.36 ± 0.68
F07	418	140	9,409	2,950	22.51 ± 0.70
F08	425	154	8,584	3,084	20.20 ± 0.82
F09	147	127	2,993	2,563	20.36 ± 0.71
F10	369	176	6,973	3,194	18.90 ± 0.40
F11	228	57	4,813	1,172	21.11 ± 0.59
F12	91	96	1,701	1,738	18.69 ± 0.53
F13	151	86	3,271	1,840	21.66 ± 0.49
F14	275	216	4,871	3,825	17.71 ± 0.46
F15	370	198	7,369	3,913	19.92 ± 0.66
F16	271	25	5,030	413	18.56 ± 0.69
F17	281	17	5,099	297	18.15 ± 0.97

the 12 Sentinel-2 band values. From these, 75 990 rows are labeled as positive (i.e., productive crop field hexagons tracked over the period) and 30 745 as negative (i.e., nonproductive crop field hexagons tracked over the period). The number of positive hexagons representing geolocations is 5066, while the number of negative hexagons is 2050 resulting in a slightly unbalanced dataset. The number of images for each hexagon collected on different dates varies from 15 to 38, and the averages for each field are represented in the last column.

We have labeled each hexagon as positive or negative based on the productive agriculture machine operations, such as planting or harvesting. Specifically, hexagons containing evidence of these operations were labeled positive, while neighboring hexagons within a three-layer radius were labeled as negative, as shown in Fig. 2. Labeling neighboring samples as negative is particularly interesting because they are often the hardest for prediction models to classify.

One noteworthy aspect of the proposed method is its ability to distinguish nonproductive fields that share the same shape as productive ones. Even a highly skilled individual would struggle to make this distinction. The key reason behind this lies in the trained model's ability to recognize patterns of band values over time from nonproductive areas as distinctly different than productive cropped areas. This approach leads to significantly more accurate results. Fig. 3 shows an example of a nonproductive field correctly identified.

Some false negatives may occur where productive fields are not detected due to the absence of agriculture machines equipped with satellite receptors or, for many reasons, when data are not shared. However, the dataset was manually curated to minimize the number of false negatives, specifically targeting the hexagonal regions between crop and noncrop fields. Despite these efforts, some false negatives may still be present. Even so, the proposed dataset is a valuable resource for future



Fig. 2. Productive crop field filled with positively labeled hexagons in green surrounded by a three hexagons layer of inferred negative samples.



Fig. 3. Nonproductive field properly classified with red hexagons.

remote-sensing research since, to our knowledge, it is the first to offer high-quality labeled productive crop fields.

IV. BENCHMARK RESULTS

This section offers state-of-the-art ML and DL benchmark results to facilitate further comparison. We have analyzed the semisupervised classification of unlabeled data and deep neural networks with different training strategies (i.e., supervised and self-supervised learning). We can use these models to predict previously unseen hexagons or pixels based on the precision required for the output image. Both the dataset and implementation notebooks are publicly available at <https://github.com/egnascimento/productivefieldsdetection>.

A. Data Processing

We processed and grouped the data to construct bidimensional time-series samples. Each comprises 15 randomly selected image dates, as shown in Fig. 4. A total of 8342 grouped multitemporal time-series samples resulted. Selecting sparse dates throughout the year is the best strategy

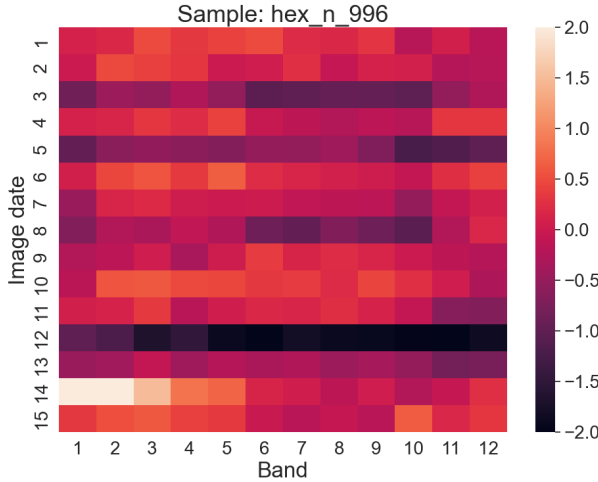


Fig. 4. Multitemporal time-series sample visualization with 15 rows (i.e., each row corresponding to a unique date a satellite image was captured of the hexagon location) and 12 columns (i.e., satellite band values).

for a comprehensive collection comprising different weather seasons and crop stages.

The original dataset was split into 80% training, 10% test, and 10% validation data keeping the balance between positive and negative labeled data.

B. ML and DL Methods

Based on the dataset's characteristics and training strategies, three state-of-the-art methods on ML and DL were chosen.

1) *Positive unlabeled (PU)* [14] is a semisupervised classification approach of unlabeled data that is particularly suitable for the current study, given the availability of accurate positive data, the lack of negative one, and the ease of obtaining unlabeled data. PU learning relies on supervised methods, and we selected support vector machines (SVMs) for this evaluation.

2) *Triplet Loss Siamese network* [25] is designed to learn representations that effectively discriminate similar and dissimilar samples in a latent space. The Triplet Loss function compares the distance between an anchor sample and a positive one against the distance between the anchor sample and a negative one.

3) *Contrastive learning* [26] is especially recommended in scenarios of limited data availability (e.g., regions with precision agriculture limited or nonexistent). Contrastive learning methods are employed to address the shortage of samples by employing data augmentation. This approach has been widely used to tackle diverse issues with significant potential for detecting crop fields. We have implemented the well-known SimCLR [27]. As contrastive learning is highly dependent on good data augmentation, a random jitter of up to $\pm 10\%$ was applied to all bands to create augmented samples.

We have implemented the DL-based neural networks using four convolutional layers with a kernel size of 3 and stride of 1, as demonstrated in Fig. 5.

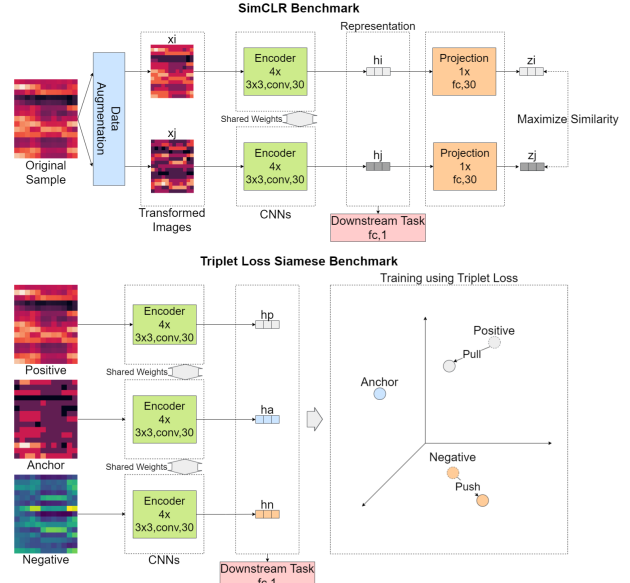


Fig. 5. Neural network architectures employed in the benchmark testing.



Fig. 6. Blue hexagons represent prediction mistakes, usually found between productive and nonfield areas.

C. Results

Table II presents the results, including metrics suitable for evaluating this problem [28]. The accuracies of PU learning, contrastive learning, and Triplet Loss Siamese were 95.36%, 97.05%, and 97.47%, respectively. PU learning achieved accuracies slightly below DL methods, a remarkable performance that can still be significantly improved by changing the underlying method to a DL neural network. The F1 score weighted average was used since the dataset is imbalanced. Additionally, we included individual F1 scores by class to demonstrate that the best results came from the more reliable samples labeled by machine data. Finally, the analysis of the Matthews correlation coefficient (MCC), appropriate to imbalanced datasets, supported the conclusion that the Triplet Loss Siamese method achieved the best overall results.

Analyzing the results, we have observed that all models missed, in most cases, the prediction of samples located between field and nonfield areas, as presented in Fig. 6. These

TABLE II
BENCHMARK RESULTS

Models	Metrics				
	Accuracy	F1-weighted	F1-Neg	F1-Pos	MCC
DL Baseline	96.62%	96.61%	94.26%	97.61%	0.92
PU SVM	95.36%	95.36%	92.27%	96.68%	0.89
C. Learning	97.05%	97.03%	94.96%	97.91%	0.93
Triplet Loss	97.47%	97.47%	95.77%	98.19%	0.94

295 mistakes, however, should not be relevant when performing
296 classification at the pixel level.

V. CONCLUSION

298 The dataset proposed in this letter represents an important
299 alternative to training highly accurate prediction models that
300 automatically detect productive crop fields. The main advantage
301 is that it does not rely on manual work, which ensures,
302 although not perfect, high-quality labeled samples in large
303 volumes since they are continuously produced by machines
304 equipped with precision agriculture devices. In sequence,
305 we evaluated three different and complementary state-of-the-
306 art ML and DL algorithms well suited to the problem of detecting
307 productive crop fields. The benchmark results present a
308 performance high enough for most real applications involving
309 detecting and delineating productive crop fields. For future
310 work, we suggest collecting more data, including different
311 crops. We also suggest improvements in the data augmentation
312 when contrastive learning is used and evaluating an instance
313 segmentation algorithm, possibly a graph-based one, which
314 should be connected to the end of the pipeline to produce
315 shape files ready-to-use by precision agriculture systems.

ACKNOWLEDGMENT

316 The authors would like to express our gratitude to
317 John Deere for generously sharing the data. This partnership
318 has reinforced the company's unwavering commitment to
319 advancing scientific research while prioritizing the confidence-
320 tiality and security of its customers' data. We appreciate this
321 collaboration and recognize the crucial role that technology
322 companies like John Deere play in supporting scientific innovation.
323 This research was supported by CNPq and FAPESP.

REFERENCES

- [1] G. Nelson et al., *Food Security, Farming, and Climate Change to 2050: Scenarios, Results, Policy Options*. Feb. 2010.
- [2] N. Zhang, M. Wang, and N. Wang, "Precision agriculture—A worldwide overview," *Comput. Electron. Agricult.*, vol. 36, pp. 113–132, Nov. 2002.
- [3] D. J. Mulla, "Twenty five years of remote sensing in precision agriculture: Key advances and remaining knowledge gaps," *Biosyst. Eng.*, vol. 114, no. 4, pp. 358–371, Apr. 2013.
- [4] I. Bhakta, S. Phadikar, and K. Majumder, "State-of-the-art technologies in precision agriculture: A systematic review," *J. Sci. Food Agricult.*, vol. 99, no. 11, pp. 4878–4888, Aug. 2019.
- [5] M. Spekken, J. P. Molin, and T. L. Romanelli, "Cost of boundary manoeuvres in sugarcane production," *Biosyst. Eng.*, vol. 129, pp. 112–126, Jan. 2015.
- [6] L. M. Griffel, V. Vazhnik, D. S. Hartley, J. K. Hansen, and M. Roni, "Agricultural field shape descriptors as predictors of field efficiency for perennial grass harvesting: An empirical proof," *Comput. Electron. Agricult.*, vol. 168, Jan. 2020, Art. no. 105088.
- [7] É. L. Bolfe et al., "Precision and digital agriculture: Adoption of technologies and perception of Brazilian farmers," *Agriculture*, vol. 10, p. 653, Dec. 2020.
- [8] A. García-Pedrero, M. Lillo-Saavedra, D. Rodríguez-Esparragón, and C. Gonzalo-Martín, "Deep learning for automatic outlining agricultural parcels: Exploiting the land parcel identification system," *IEEE Access*, vol. 7, pp. 158223–158236, 2019.
- [9] C. Persello, V. A. Tolpekin, J. R. Bergado, and R. A. de By, "Delineation of agricultural fields in smallholder farms from satellite images using fully convolutional networks and combinatorial grouping," *Remote Sens. Environ.*, vol. 231, Sep. 2019, Art. no. 111253.
- [10] K. M. Masoud, C. Persello, and V. A. Tolpekin, "Delineation of agricultural field boundaries from Sentinel-2 images using a novel super-resolution contour detector based on fully convolutional networks," *Remote Sens.*, vol. 12, no. 1, p. 59, Dec. 2019.
- [11] F. Waldner and F. I. Diakogiannis, "Deep learning on edge: Extracting field boundaries from satellite images with a convolutional neural network," *Remote Sens. Environ.*, vol. 245, Aug. 2020, Art. no. 111741.
- [12] F. Waldner et al., "Detect, consolidate, delineate: Scalable mapping of field boundaries using satellite images," *Remote Sens.*, vol. 13, p. 2197, Jun. 2021.
- [13] M. P. Wagner and N. Oppelt, "Extracting agricultural fields from remote sensing imagery using graph-based growing contours," *Remote Sens.*, vol. 12, no. 7, p. 1205, Apr. 2020.
- [14] F. Denis, R. Gilleron, and F. Letouzey, "Learning from positive and unlabeled examples," *Theor. Comput. Sci.*, vol. 348, no. 1, pp. 70–83, Dec. 2005.
- [15] R. Guldenring and L. Nalpantidis, "Self-supervised contrastive learning on agricultural images," *Comput. Electron. Agricult.*, vol. 191, Dec. 2021, Art. no. 106510.
- [16] S. Crommelinck, M. Koeva, M. Y. Yang, and G. Vosselman, "Application of deep learning for delineation of visible cadastral boundaries from remote sensing imagery," *Remote Sens.*, vol. 11, no. 21, p. 2505, Oct. 2019.
- [17] R. Yang, Z. U. Ahmed, U. C. Schulthess, M. Kamal, and R. Rai, "Detecting functional field units from satellite images in smallholder farming systems using a deep learning based computer vision approach: A case study from Bangladesh," *Remote Sens. Appl., Soc. Environ.*, vol. 20, Nov. 2020, Art. no. 100413.
- [18] H. C. North, D. Pairman, and S. E. Belliss, "Boundary delineation of agricultural fields in multitemporal satellite imagery," *IEEE J. Sel. Topics Appl. Earth Observ. Remote Sens.*, vol. 12, no. 1, pp. 237–251, Jan. 2019.
- [19] C. Evans, R. Jones, I. Svalbe, and M. Berman, "Segmenting multispectral Landsat TM images into field units," *IEEE Trans. Geosci. Remote Sens.*, vol. 40, no. 5, pp. 1054–1064, May 2002.
- [20] A. García-Pedrero, C. Gonzalo-Martín, and M. Lillo-Saavedra, "A machine learning approach for agricultural parcel delineation through agglomerative segmentation," *Int. J. Remote Sens.*, vol. 38, no. 7, pp. 1809–1819, Apr. 2017.
- [21] C. Seiffert, T. M. Khoshgoftaar, J. Van Hulse, and A. Napolitano, "RUSBoost: A hybrid approach to alleviating class imbalance," *IEEE Trans. Syst., Man, Cybern. A, Syst. Humans*, vol. 40, no. 1, pp. 185–197, Jan. 2010.
- [22] N. Kussul, M. Lavreniuk, S. Skakun, and A. Shelestov, "Deep learning classification of land cover and crop types using remote sensing data," *IEEE Geosci. Remote Sens. Lett.*, vol. 14, no. 5, pp. 778–782, May 2017.
- [23] A. García-Pedrero, C. Gonzalo-Martín, M. Lillo-Saavedra, and D. Rodríguez-Esparragón, "The outlining of agricultural plots based on spatiotemporal consensus segmentation," *Remote Sens.*, vol. 10, no. 12, p. 1991, Dec. 2018.
- [24] M. P. Wagner and N. Oppelt, "Deep learning and adaptive graph-based growing contours for agricultural field extraction," *Remote Sens.*, vol. 12, no. 12, p. 1990, Jun. 2020.
- [25] F. Schroff, D. Kalenichenko, and J. Philbin, "FaceNet: A unified embedding for face recognition and clustering," in *Proc. IEEE Comput. Soc. Conf. Comput. Vis. Pattern Recognit.*, Jun. 2015, pp. 815–823.
- [26] A. Jaiswal, A. R. Babu, M. Z. Zadeh, D. Banerjee, and F. Makedon, "A survey on contrastive self-supervised learning," *Technologies*, vol. 9, no. 1, p. 2, Dec. 2020.
- [27] T. Chen, S. Kornblith, M. Norouzi, and G. Hinton, "A simple framework for contrastive learning of visual representations," in *Proc. 37th ICML*, 2020, pp. 1597–1607.
- [28] Z. Zhang, Q. Liu, and Y. Wang, "Road extraction by deep residual U-Net," *IEEE Geosci. Remote Sens. Lett.*, vol. 15, no. 5, pp. 749–753, May 2018.